Chapter 14

ENAMEL THICKNESS IN THE SCLADINA I-4A NEANDERTAL TEETH

Stefano BENAZZI, Michel TOUSSAINT & Jean-Jacques HUBLIN

Michel Toussaint & Dominique Bonjean (eds.), 2014.
The Scladina I-4A Juvenile Neandertal (Andenne, Belgium),
Palaeoanthropology and Context
Études et Recherches Archéologiques de l'Université de Liège, 134: 307-314.

1. Introduction

Over the past century, the enamel thickness has been extensively used for the taxonomic, phylogenetic, and dietary assessment of extant and fossil primates, and is considered an effective dental feature to distinguish between the thickly-enameled hominin taxa and the relatively thin-enameled extant African apes (e.g., Molnar & Gantt, 1977; Schwartz, 2000; Martin et al., 2003; Grine et al., 2005; Olejniczak et al., 2007; Vogel et al., 2008).

Even though a general overlap in enamel thickness range of variation characterizes the genus *Homo* (Smith et al., 2012), it has been observed that recent and fossil *Homo sapiens* possess absolutely and relatively thicker enamel than *Homo neanderthalensis* (Olejniczak et al., 2008; Benazzi et al., 2011[a]; Smith et al., 2012). These findings mainly depend on differences in both dental topography and tissue proportions, since Neandertals have more complex enamel-dentine junction (EDJ) surface and larger dentine volume than *Homo sapiens*, resulting in lower average and relative enamel thickness (e.g., Macchiarelli et al., 2006; Smith et al., 2007; 2012; Olejniczak et al., 2008; Bayle et al., 2009[a,b], 2010; Benazzi et al., 2011[a]). Nonetheless, some contributions reported a Neanderthal enamel thickness in the range of *Homo sapiens* (Benazzi et al., 2011[b,c], 2013). This might be due to methodological shortcomings of previous techniques to compute the enamel thickness (Benazzi et al., 2014). In addition, the real Neandertal range of variation is not yet clearly understood.

With regard to the methodology, preliminary studies on the enamel thickness considered physical cross-sections of molar teeth (e.g., Molnar & Gantt, 1977; Martin, 1985; Schwartz, 2000; Grine, 2004, 2005; Grine et al., 2005), but concerns have been raised about its destructive nature, as well as problems related to specimen orientation and the reductive information carried by the two-dimensional (2D) enamel cap morphology when compared with the more complex three-dimensional (3D) shape of the crown (Olejniczak, 2006). Therefore, non-destructive techniques based on micro-computed tomography (micro-CT) were proposed to refine the 2D enamel thickness analysis and, most importantly, to study the thicknesses of dental enamel in its full 3D form (Olejniczak, 2006, followed by Olejniczak et al., 2008). However, it has been recently emphasized that the suggested digital approaches have some methodological flaws and can only be applied to molar teeth, thus explaining the reason for the low number of studies on premolars and anterior teeth (Feeney et al., 2010; Smith et al., 2012). In a recent contribution Benazzi and colleagues (2014) addressed this issue, providing rigorous guidelines for the digital computation of 2D and 3D enamel thickness in molars, premolars, canines and incisors.

The enamel thickness variation in Neandertal teeth is difficult to assess. The 2D and mainly the 3D enamel thickness analyses require unworn or slightly worn teeth, which are much less frequent in the fossil record than worn teeth. Teeth are often affected by a certain amount of wear and there is no tool, physical or digital, that can be used confidently to restore the internal and external original shape of heavily worn crowns. This is why unworn or slightly worn teeth such as those from the Scladina dental sample are of particular value for the investigation of enamel thickness variability.

In this contribution we provide the components of 2D and 3D enamel thickness of the Scladina molars, premolars and canines using a new approach recently standardized by Benazzi and colleagues (2014). We aim to improve our understanding of the Neandertal range of variation for the enamel thickness, and then to promote the comparison of the results.

2. Materials and methods

Thirteen Neandertal teeth from Scladina, Belgium, were considered to compute the components of 2D and 3D enamel thickness. Most of the teeth are unworn or slightly worn, except for three first molars that show moderate dentine exposure (wear stage 3, based on Smith, 1984). A list of the Scladina teeth included in the analysis, as well as their wear stage, is reported in Tables 1 & 2.

The teeth were scanned with a Skyscan 1172 micro-CT (Max Planck Institute for Evolutionary Anthropology, Leipzig, Germany) using the following scan parameters: 100kV, 100µA, with an aluminum/copper filter (0.5 mm/0.04 mm thickness). Volume data were reconstructed using isometric voxels of 13.74 µm. Each image stack was segmented using a semiautomatic threshold-based approach in Avizo 7 (Visualization Sciences Group Inc.) to separate the enamel, the dentine and the pulp chamber and to reconstruct 3D digital models from the tooth volume data.

Following guidelines underlined by Benazzi et al. (2014), the digital models were then imported in Rapidform XOR2 (INUS Technology Incorporated, Seoul, Korea), and for each tooth class a specific protocol was used to compute both the 2D and 3D enamel thickness. As already emphasized by Olejniczak and colleagues (2008), discrepancies are observed between 3D and 2D data due to the dimensional loss in the latter. Since the 3D approach registers variation in enamel thickness across the tooth crown, the 3D data are more appropriate than 2D data. However, because the latter have been widely used to study hominoid teeth (e.g., Smith et al., 2006; 2012), in this contribution we also provide the values of the components of 2D enamel thickness.

In molars and second premolars, the cervical line was digitized using a spline curve and the best-fit plane through the points of the curve was computed (cervical plane) to separate the crown (enamel cap and dentine core) from the root (Figures 1 & 2).

For the 3D analysis of molars and second premolars, the following measurements were obtained from the crown: the volume of the enamel cap (mm^3); the volume of the dentine core (which includes the volume of the coronal pulp – mm^3); the enamel-dentine junction (EDJ) surface (the interface between the enamel cap and the dentine core – mm^2). These measurements were used for the computation of both the 3D average enamel thickness index (3D AET = volume of enamel divided by the EDJ surface; index in millimetres) and the 3D relative enamel thickness index (3D RET = 3D AET divided by the cubic root of dentine volume; scale-free index).

For the 2D analysis of molars and second premolars, a digital cross-section perpendicular to the cervical plane and passing through the two mesial (mesial section) dentine horn tips (paracone and protocone in permanent maxillary molars; protoconide and metaconide in permanent mandibular molars/second premolars) was created. Then, a line was digitized to join the most buccal and lingual apical extension of enamel (Figures 1 & 2). The following measurements were recorded from the sections: the area of the enamel

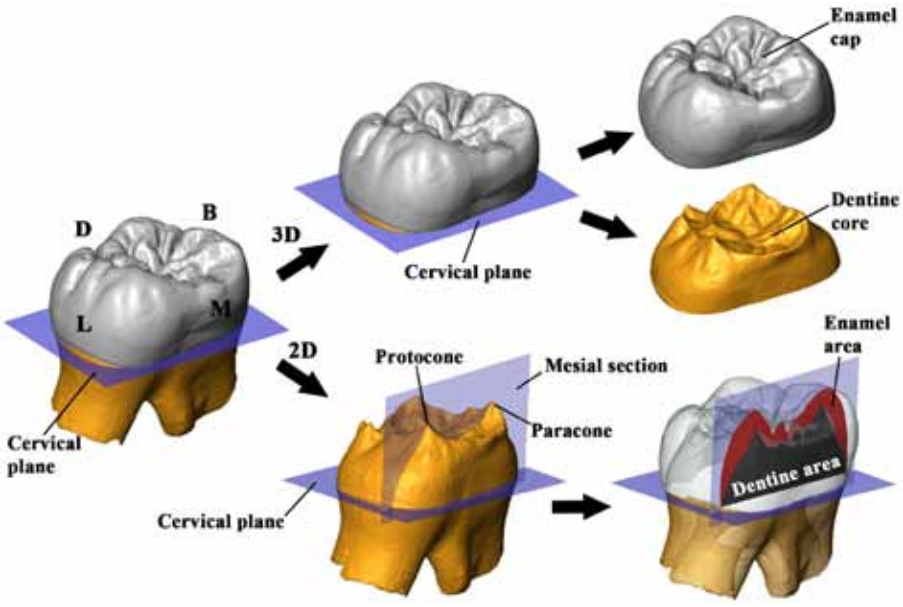

Figure 1: On the left, a best-fit plane (cervical plane) was computed on the cervical line of Scla 4A-3 permanent maxillary right second molar (RM^2). For 2D enamel thickness, the mesial section is perpendicular to the cervical plane and passes through the mesial (paracone and protocone) dentine horn tips. In the 3D enamel thickness, the crown is separated from the root based on the cervical plane to identify the enamel cap and the dentine core of the crown. B = buccal; D = distal; L = lingual; M = mesial.

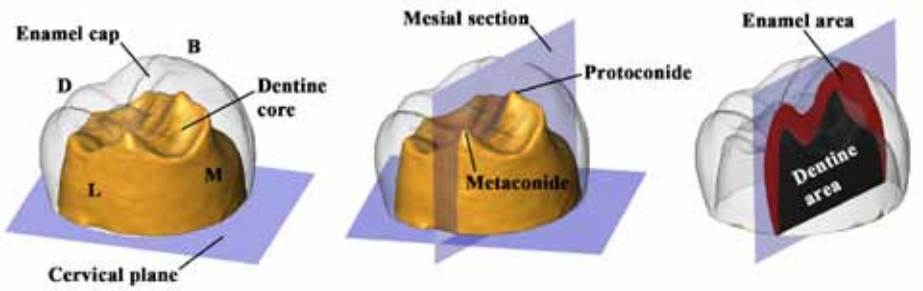

Figure 2: On the left, a best-fit plane (cervical plane) was computed on the cervical line of Scla 4A-9/P_4 mandibular left second premolar to separate the crown from the root; the enamel cap, the dentine core, and the interface between them (enamel-dentine junction (EDJ) surface) were used for the computation of the 3D enamel thickness indices. For 2D enamel thickness, the mesial section is perpendicular to the cervical plane and passes through the mesial (protoconide and metaconide) dentine horn tips.

cap (mm²); the area of the coronal dentine (mm²), which includes the coronal pulp; the length of the EDJ (the linear interface between the enamel area and the dentine area – mm); the 2D average enamel thickness index (2D AET = the area of the enamel cap divided by the length of the EDJ; index in millimetres); the 2D relative enamel thickness index (2D RET = 2D AET divided by the square root of the coronal dentine area; scale-free index).

In the 3D analysis of first premolars and canines the coronal dentine was separated from the root dentine based on the curve digitized on the cervical line. The smooth surface interpolating the curve was then used to seal the digital model of the dentine core (Figures 3 & 4).

In the 2D analysis of first premolars, a virtual section of the tooth perpendicular to the best-fit plane of the cervical line (cervical plane) and passing through the main dentine horn tips (protoconide and metaconide in mandibular first premolars; paracone and protocone in maxillary first premolars) was created (Figure 3). Instead, each canine was oriented in its anatomical position to visualize the buccal and lingual sides. A virtual section was created passing through two

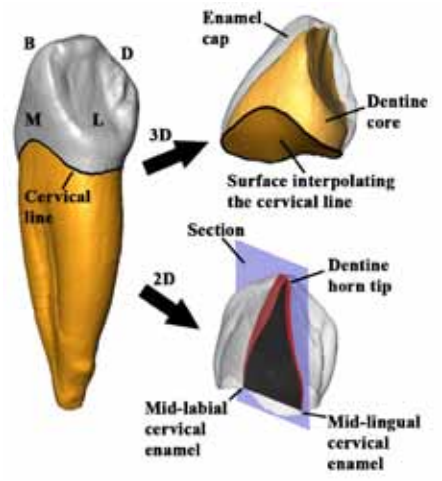

Figure 4: On the left, a spline curve (black) was digitized on the cervical line of Scla 4A-12 permanent mandibular right canine (RC_1). For 3D enamel thickness, the coronal dentine was separated from the root dentine based on the cervical line, which was then interpolated by a smooth surface to seal the bottom of the dentine core. For 2D enamel thickness, the cross-section passes through two points digitized on the mid-labial and mid-lingual cervical enamel, respectively, and one point digitized on the dentine horn tip. B = buccal; D = distal; L = lingual; M = mesial.

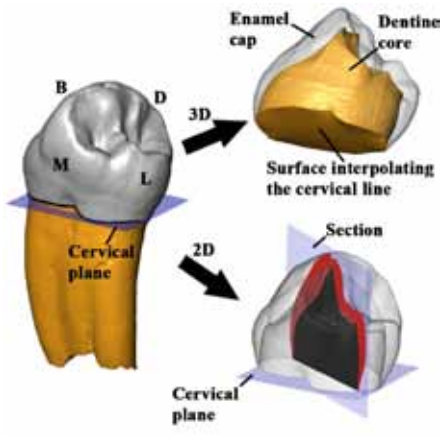

Figure 3: On the left, a spline curve (black) was digitized on the cervical line of Scla 4A-6 mandibular right first premolar (RP_3). For the 2D enamel thickness, the best-fit plane of the curve was computed (cervical plane), and a mesial section perpendicular to this plane and passing through the mesial (protoconide and metaconide) dentine horn tips was created. For the 3D enamel thickness, the coronal dentine was separated from the root dentine based on the cervical line, which was then interpolated by a smooth surface to seal the bottom of the dentine core. B = buccal; D = distal; L = lingual; M = mesial.

points digitized on the mid-labial and mid-lingual cervical enamel, respectively, and the dentine horn tip (Figure 4). In both first premolars and canines, a line was then digitized to join the most buccal and lingual apical extension of enamel. The computation of the AET and RET indices (both in 2D and 3D) follows indications mentioned above.

Comparative data for 2D and 3D enamel thickness for Neandertals and *Homo sapiens* were sourced from Smith et al. (2006; 2012) and Olejniczak et al. (2008). When possible, for 2D data standardized score (Z-scores) values were computed to establish whether the values obtained for the Scladina teeth were closest to either the Neandertal or *Homo sapiens* group mean. However, since the comparative data were obtained using approaches that have been recently refined by Benazzi et al. (2014), who recognized shortcomings in the protocol of tooth orientation, we emphasize that the comparison should be considered tentative at best.

3. Results

The values of the components of 2D and 3D enamel thickness, as well as the AET and RET indices for the 13 Scladina Neandertal teeth are shown in Tables 1 & 2. Results obtained for the first molars should be considered with caution, because tooth wear (wear stage 3 based on Smith, 1984) affects much more the enamel than the dentine, so that the computed AET and RET indices are certainly lower than the indices we would have computed for the unworn teeth. While in some cases 2D and 3D indices supply similar results, in other circumstances differences between the two approaches are quite noticeable (e.g., Scla 4A-1/P_4, Scla 4A-2/P^3, Scla 4A-9/P_4, Scla 4A-16 RC^1). Interestingly, it seems that the discrepancy between 2D and 3D data increases in premolars and anterior teeth when compared with molars, but this tendency might be biased by the small sample size. In any case, as mentioned above, 3D data (Table 2) are more suitable than 2D data (Table 1).

Based on 3D data of the unworn/slightly worn teeth (Table 2), premolars have generally larger RET index than molars (premolars = 20.89±2.45; molars = 18.61±0.69), but the condition is reversed for the AET index (premolars = 1.08±0.11; molars = 1.20±0.04). The canines show the lowest values, both for AET (0.77±0.11) and RET (13.44±1.03) indices, having absolutely and relatively little enamel surrounding a large bulk of dentine. Similar results are observed in the 2D data, at least for the AET indices (molars = 1.16±0.08; premolars = 1.0±0.06; canines = 0.69±0.1) and the canine RET indices (canines = 10.43±0.7) (Table 1). However, a reverse condition, when compared with 3D data, characterizes the mean 2D RET indices computed for molars (19.44±1.74) and premolars (17.58±1.59). Therefore, results obtained for canines and molars are more consistent between 2D and 3D analysis than results obtained for premolars.

When the Scladina molars are compared with AET and RET mean values (both 2D and 3D) computed for Neandertals and *Homo sapiens*, results are ambiguous. When the three most worn first molars are excluded (their low indices ally them with Neandertal but might well be an artefact

Scladina specimens	Tooth class	Enamel area (mm^2)	Coronal area (mm^2)	EDJ length (mm)	AET (mm)	RET (scale-free)	Wear stage[a]
Scla 4A-1/P_4	RP_4	17.75	31.09	17.51	1.01	18.18	1
Scla 4A-1/M_1	RM_1	15.58	37.16	18.01	0.86	14.19	3
Scla 4A-1/M_2	RM_2	19.92	36.78	18.78	1.06	17.49	1
Scla 4A-1/M_3	RM_3	19.74	32.10	17.10	1.15	20.38	unworn
Scla 4A-2/P^3	RP^3	19.98	38.03	19.16	1.04	16.91	unworn
Scla 4A-3	RM^2	22.14	38.11	19.33	1.15	18.56	unworn
Scla 4A-4	RM^1	17.19	39.41	19.00	0.90	14.41	3
Scla 4A-6	RP_3	16.14	33.81	17.59	0.92	15.78	unworn
Scla 4A-9/ P_4	LP_4	17.48	28.58	16.81	1.04	19.45	1
Scla 4A-9/ M_1	LM_1	15.08	39.57	18.16	0.83	13.20	3
Scla 4A-9/ M_2	LM_2	22.81	35.12	18.03	1.26	21.34	unworn
Scla 4A-12	RC_1	12.53	38.38	20.35	0.62	9.94	1
Scla 4A-16	RC^1	16.83	47.95	22.24	0.76	10.93	unworn

Table 1: Values of the components of two-dimensional (2D) enamel thickness measurements in the Scladina teeth ([a]based on Smith (1984); EDJ = enamel dentine junction; AET = average enamel thickness; RET = relative enamel thickness).

Scladina specimens	Tooth class	Enamel volume (mm^3)	Coronal dentine + pulp volume (mm^3)	EDJ surface (mm^2)	AET (mm)	RET (scale-free)	Wear stage[a]
Scla 4A-1/P_4	RP_4	134.54	131.12	116.88	1.15	22.66	1
Scla 4A-1/M_1	RM_1	198.26	285.73	202.97	0.98	14.83	3
Scla 4A-1/M_2	RM_2	229.69	275.63	197.00	1.17	17.92	1
Scla 4A-1/M_3	RM_3	209.91	230.14	175.59	1.20	19.51	unworn
Scla 4A-2/P^3	RP^3	142.53	149.72	128.98	1.11	20.81	unworn
Scla 4A-3	RM^2	228.29	264.81	194.67	1.17	18.26	unworn
Scla 4A-4	RM^1	219.65	286.69	201.23	1.09	16.55	3
Scla 4A-6	RP_3	120.58	144.40	131.68	0.92	17.45	unworn
Scla 4A-9/ P_4	LP_4	132.99	127.69	116.65	1.14	22.64	1
Scla 4A-9/ M_1	LM_1	194.59	300.40	209.21	0.93	13.89	3
Scla 4A-9/ M_2	LM_2	257.35	297.81	205.66	1.25	18.74	unworn
Scla 4A-12	RC_1	99.56	160.67	144.11	0.69	12.71	1
Scla 4A-16	RC^1	145.16	215.02	170.99	0.85	14.17	unworn

Table 2: Values of the components of three-dimensional (3D) enamel thickness measurements in the Scladina teeth ([a]based on Smith (1984); EDJ = enamel dentine junction; AET = average enamel thickness; RET = relative enamel thickness).

Tooth class			AET			RET		
	Sample	N	Mean (SD)	Min–Max	Z–score	Mean (SD)	Min–Max	Z–score
M^1	N	3[a]	1.05 (0.13)	0.93–1.19		15.37 (1.57)	13.8–16.93	
	FHS	4[b]	1.28	1.08–1.58		18.2	15.7–20.9	
	RHS	37[c]	1.22 (0.12)	0.98–1.5		18.75 (2.08)	13.95–23.86	
	Scla 4A-4		**0.90**		**N=–1.15 RHS=–2.67**	**14.41**		**N=–0.61 RHS=–2.09**
M^2	N	5[a]	1.21 (0.08)	1.13–1.29		18.18 (2.05)	15.65–20.85	
	FHS	1[b]	1.31			19.8		
	RHS	25[c]	1.40 (0.17)	1.13–1.76		21.59 (3.13)	16.49–28.03	
	Scla 4A-3		**1.15**		**N=–0.75 RHS=–1.47**	**18.56**		**N=0.19 RHS=–0.97**
M_1	N	12[a]	1.01 (0.07)	0.93–1.18		16.06 (1.64)	13.77–20.46	
	FHS	6[b]	1.19	0.96–1.47		18.0	15.2–23.3	
	RHS	55[c]	1.07 (0.13)	0.8–1.4		16.99 (2.29)	11.76–22.62	
	Scla 4A-1/M_1		0.86		N=–2.14 RHS=–1.62	14.19		N=–1.14 RHS=–1.22
	Scla 4A-9/M_1		**0.83**		**N=–2.57 RHS=–1.85**	**13.20**		**N=–1.74 RHS=–1.66**
M_2	N	6[a]	1.02 (0.08)	0.94–1.14		15.63 (0.87)	14.21–16.8	
	FHS	4[b]	1.28	1.17–1.41		18.3	16.3–20.2	
	RHS	45[c]	1.19 (0.14)	0.94–1.55		20.51 (2.93)	14.85–27.66	
	Scla 4A-1/M_2		**1.06**		**N=0.5 RHS=–0.93**	**17.49**		**N=2.14 RHS=–1.03**
	Scla 4A-9/M_2		**1.26**		**N=3 RHS=0.5**	**21.34**		**N=6.56 RHS=0.28**
M_3	N	8[a]	0.99 (0.06)	0.92–1.1		16.55 (1.28)	14.3–18.34	
	FHS	2[b]	1.28	1.15–1.41		20.5	19.2–21.9	
	RHS	44[c]	1.24 (0.15)	0.98–1.67		21.63 (2.99)	17.22–31.84	
	Scla 4A-1/M_3		**1.15**		**N=2.67 RHS=–0.6**	**20.38**		**N=2.99 RHS=–0.42**

Table 3: Two-dimensional (2D) enamel thickness in the Scladina molar sample, compared with mean value indices computed in Neandertal (N), fossil *Homo sapiens* (FHS) and recent *Homo sapiens* (RHS); when possible, standard deviation (SD), minimum-maximum values and standardized Z-scores are provided. Data from [a]Olejniczak et al. (2008), [b]Smith et al. (2012), [c]Smith et al. (2006).

of tooth wear), the Scladina teeth (particularly for the RET index) generally fall on the higher end or even outside the Neandertal range of variation, often in between the currently known Neandertal and *Homo sapiens* mean values (Tables 3 & 4).

The paucity of comparative data for premolars and canines (Smith et al., 2012), which are only in 2D, and the incompleteness of statistic information given (e.g., standard deviation and range values are not provided), limit us in the

Tooth class			AET		RET	
	Sample	n	Mean (SD)	Min–Max	Mean (SD)	Min–Max
M^1	N	1	1.07		15.13	
	RHS	6	1.13		17.05	
	Scla 4A-4		**1.09**		**16.55**	
M^2	N	4	1.07 (0.08)	0.97–1.14	15.33 (1.83)	13.65–17.56
	RHS	6	1.46		23.36	
	Scla 4A-3		**1.17**		**18.26**	
M_1	N	9	1.17 (0.23)	0.97–1.63	16.77 (3.8)	13.03–24.02
	RHS	1	1.05		15.87	
	Scla 4A-1/M_1		**0.98**		**14.83**	
	Scla 4A-9/M_1		**0.93**		**13.89**	
M_2	N	4	0.99 (0.11)	0.89–1.13	13.63 (0.47)	13.13–14.18
	RHS	9	1.46		23.44	
	Scla 4A-1/M_2		1.17		17.92	
	Scla 4A-9/M_2		1.25		18.74	
M_3	N	6	1.06 (0.20)	0.82–1.3	15.43 (2.82)	12.74–19.67
	RHS	9	1.45		23.79	
	Scla 4A-1/M_3		**1.20**		**19.51**	

Table 4: Three-dimensional (3D) enamel thickness in the Scladina molar sample, compared with mean value indices computed in Neandertal (N) and recent *Homo sapiens* (RHS); when possible, standard deviation (SD) and minimum-maximum values are provided (data from Olejniczak et al., 2008).

Tooth class	Taxon	n	AET (mean)	RET (mean)
RC^1	FHS	2	0.87	12.71
	RHS	22	0.91	14.43
	Scla 4A-16		**0.76**	**10.93**
RC_1	FHS	4	0.77	10.65
	RHS	20	0.81	12.91
	Scla 4A-12		**0.62**	**9.94**
RP^3	FHS	1	1.26	18.74
	RHS	19	1.1	17.69
	Scla 4A-2/P^3		**1.04**	**16.91**
RP_3	FHS	3	1.04	15.81
	RHS	17	1.01	17.78
	Scla 4A-6		**0.92**	**15.78**
LP_4	FHS	2	1.08	16.17
	RHS	17	1.20	21.19
	Scla 4A-1/P_4		**1.01**	**18.18**
	Scla 4A-9/P_4		**1.04**	**19.45**

Table 5: Two-dimensional (2D) enamel thickness in the Scladina canine and premolar sample, compared with mean value indices computed in fossil *Homo sapiens* (FHS) and recent *Homo sapiens* (RHS); data from Smith et al. (2012).

discussion of the results obtained for the Scladina enamel thickness. However, we can summarize our findings as follows: the low AET values of the Scladina premolars and canines find more correspondence with Neandertal than *Homo sapiens* mean values (Table 5). Similarly, the low RET index of the canines is in agreement with values observed in Neandertal, while results computed for the premolars are more ambiguous, but this is certainly due to the extremely small Neandertal comparative sample size.

4. Discussion and conclusions

As absence of wear is an essential precondition to compute the values for 2D and 3D enamel thickness, the unworn/slightly worn Scladina teeth represent a valuable sample for the advancement of our knowledge on Neandertal's enamel thickness variability.

It is generally accepted that Neandertals had a lower average and relative enamel thicknesses than *Homo sapiens*, (e.g. Macchiarelli et al., 2006; Smith et al., 2007, 2012; Olejniczak et al., 2008; Bayle et al., 2009[a,b], 2010), but shortcomings observed in previous methods might have contributed to the confusing result and misrepresent the real range of enamel thickness variation. Results obtained for the Scladina teeth point out that indeed Neandertals have lower AET and RET indices than *Homo sapiens*, but they also suggest that the discrepancy observed in previous studies between the two groups (e.g. Smith et al., 2006, 2012; Olejniczak et al., 2008) has been overemphasized, as recently observed by Benazzi and colleagues (2011[c], 2013[a]). This does not mean that Neandertals and *Homo sapiens* overlap in AET and RET indices, but it suggests that the Neandertal range of variation is still unknown. This issue could be solved using rigorous and consistent methodological protocols in large *Homo sapiens* (recent and fossil) and Neandertal dental samples.

This contribution is one of the few providing 2D enamel thickness for premolars and canines

(see also Feeney et al., 2010; Smith et al., 2012), and the first providing 3D enamel thickness for these dental classes. With regard to the 3D data, our results suggest that molars, premolars and canines (and presumably incisors) have a different and peculiar trend, with premolars having a generally larger RET index than molars, and canines showing the lowest values. Moreover, our results confirm that Neandertal canines have lower AET and RET indices than *Homo sapiens* canines, as previously suggested by 2D data (Smith et al., 2012).

We are confident that the values of the components of 2D and 3D enamel thickness measurements reported in this paragraph for the Scladina teeth (Tables 1 & 2), coupled with a thorough explanation of the method, will be useful to favor future comparative studies between Neandertal and *Homo sapiens*, making scholars aware of the importance to increase the sample size to evaluate the enamel thickness range of variation of these two human groups.

Acknowledgements

This research was supported by the Max Planck Society.

References

Bayle P., Braga J., Mazurier A. & Macchiarelli R., 2009[a]. Dental developmental pattern of the Neanderthal child from Roc de Marsal: a high-resolution 3D analysis. *Journal of Human Evolution*, 56: 66–75.

Bayle P., Braga J., Mazurier A. & Macchiarelli R., 2009[b]. Brief communication: high-resolution assessment of the dental developmental pattern and characterization of tooth tissue proportions in the late Upper Paleolithic child from La Madeleine, France. *American Journal of Physical Anthropology*, 138: 493–498.

Bayle P., Macchiarelli R., Trinkaus E., Duarte C., Mazurier A. & Zilhão J., 2010. Dental maturational sequence and dental tissue proportions in the early Upper Paleolithic child from Abrigo do Lagar Velho, Portugal. *Proceedings of the National Academy Science of the United States of America*, 107, 4: 1338–1342.

Benazzi S., Bailey S. E. & Mallegni F., 2013. A morphometric analysis of the Neandertal upper second molar Leuca I. *American Journal of Physical Anthropology*, 152: 300–305.

Benazzi S., Douka K., Fornai C., Bauer C. C., Kullmer O., Svoboda J., Pap I., Mallegni F., Bayle P., Coquerelle M., Condemi S., Ronchitelli A., Harvati K. & Weber G. W., 2011[a]. Early dispersal of modern humans in Europe and implications for Neanderthal behaviour. *Nature*, 479: 525–528.

Benazzi S., Fornai C., Bayle P., Coquerelle M., Kullmer O., Mallegni F. & Weber G. W., 2011[b]. Comparison of dental measurement systems for taxonomic assignment of Neanderthal and modern human lower second deciduous molars. *Journal of Human Evolution*, 61: 320–326.

Benazzi S., Panetta D., Toussaint M., Gruppioni G. & Hublin J.-J., 2014. Guidelines for the digital computation of 2D and 3D enamel thickness. *American Journal of Physical Anthropology*, 153: 305–313.

Benazzi S., Viola B., Kullmer O., Fiorenza L., Harvati K., Paul T., Gruppioni G., Weber G. W. & Mallegni F., 2011[c]. A reassessment of the Neanderthal teeth from Taddeo cave (southern Italy). *Journal of Human Evolution*, 61: 377–387.

Feeney R. N. M., Zermeno J. P., Reid D. J., Nakashima S., Sano H., Bahar A., Hublin J.-J. & Smith T. M., 2010. Enamel thickness in Asian human canines and premolars. *Anthropological Science*, 118: 191–198.

Grine F. E., 2004. Geographic variation in tooth enamel thickness does not support Neandertal involvement in the ancestry of modern Europeans. *South African Journal of Science*, 100: 389–394.

Grine F. E., 2005. Enamel thickness of deciduous and permanent molars in modern *Homo sapiens*. *American Journal of Physical Anthropology*, 126: 14–31.

Grine F. E., Spencer M. A., Demes B., Smith H. F., Strait D. S. & Constant D. A., 2005. Molar enamel thickness in the chacma baboon, *Papio ursinus* (Kerr, 1792). *American Journal of Physical Anthropology*, 128: 812–822.

Macchiarelli R., Bondioli L., Debénath A., Mazurier A., Tournepiche J.-F., Birch W. & Dean C., 2006. How Neanderthal molar teeth grew. *Nature*, 444: 748–751.

Martin L. B., 1985. Significance of enamel thickness in hominoid evolution. *Nature*, 314: 260–263.

Martin L. B., Olejniczak A. J. & Maas M. C., 2003. Enamel thickness and microstructure in pitheciin primates, with comments on dietary adaptations of the middle Miocene hominoid Kenyapithecus. *Journal of Human Evolution*, 45: 351–367.

Molnar S. & Gantt D. G., 1977. Functional implications of primate enamel thickness. *American Journal of Physical Anthropology*, 46: 447–454.

Olejniczak A. J., 2006. *Micro-Computed Tomography of Primate Molars*. Unpublished PhD thesis. Stony Brook University.

Olejniczak A. J., Gilbert C. C., Martin L. B., Smith T. M., Ulhaas L. & Grine F. E., 2007. Morphology of the enamel-dentine junction in sections of anthropoid primate maxillary molars. *Journal of Human Evolution*, 53: 292–301.

Olejniczak A. J., Smith T. M., Feeney R. N. M., Macchiarelli R., Mazurier A., Bondioli L., Rosas A., Fortea J., de la Rasilla M., Garcia-Tabernero A., Radovčić J., Skinner M. M., Toussaint M. & Hublin J.-J., 2008. Dental tissue proportions and enamel thickness in Neandertal and modern human molars. *Journal of Human Evolution*, 55: 12–23.

Schwartz G. T., 2000. Taxonomic and functional aspects of the patterning of enamel thickness distribution in extant large-bodied hominoids. *American Journal of Physical Anthropology*, 111: 221–244.

Smith B. H., 1984. Patterns of molar wear in hunter-gatherers and agriculturalists. *American Journal of Physical Anthropology*, 63: 39–56.

Smith T. M., Olejniczak A. J., Reid D. J., Ferrell R. J. & Hublin J.-J., 2006. Modern human molar enamel thickness and enamel-dentine junction shape. *Archives of Oral Biology*, 51: 974–995.

Smith T. M., Olejniczak A. J., Zermeno J. P., Tafforeau P. T., Skinner M. M., Hoffmann A., Radovčić J., Toussaint M., Kruszynski R., Menter C., Moggi-Cecchi J., Glasmacher U. A., Kullmer O., Schrenk F., Stringer C. B. & Hublin J.-J., 2012. Variation in enamel thickness within the genus Homo. *Journal of Human Evolution*, 62: 395-411.

Smith T. M., Toussaint M., Reid D. J., Olejniczak A. J. & Hublin J.-J., 2007. Rapid dental development in a Middle Paleolithic Belgian Neanderthal. *Proceedings of the National Academy Science of the United States of America*, 104, 51: 20220–20225.

Vogel E. R., van Woerden J. T., Lucas P. W., Utami Atmoko S. S., van Schaik C. P. & Dominy N. J., 2008. Functional ecology and evolution of hominoid molar enamel thickness: Pan troglodytes schweinfurthii and Pongo pygmaeus wurmbii. *Journal of Human Evolution*, 55: 60–74.